Original Article

DOI: 10.5582/bst.2024.01211

Evaluation of the value of *Synechococcus* 7942 as a sensitizer for photo-sonodynamic therapy against breast cancer

Ruimei Zhao[1,2,§], Pengfei Zhao[3,§,*], Ziyuan Zhou[4,§], Deliang Liu[3,§], Yang Zhou[3], Mingbin Zheng[3,5,*], Tetsuya Asakawa[3,*], Xin Kuang[1,*]

[1] Department of Anesthesiology, People's Hospital of Longhua, Shenzhen, Guangdong Province, China;
[2] Department of Anesthesiology, Hunan Aerospace Hospital, Changsha, Hunan Provence, China;
[3] Institute of Neurology, National Clinical Research Center for Infectious Diseases, Shenzhen Third People's Hospital, Shenzhen, Guangdong Province, China;
[4] National Cancer Center, National Clinical Research Center for Cancer, Cancer Hospital & Shenzhen Hospital, Chinese Academy of Medical Sciences and Peking Union Medical College, Shenzhen, Guangdong Province, China;
[5] Key Laboratory for Nanomedicine, Guangdong Medical University, Dongguan, Guangdong, Guangdong Province, China.

SUMMARY This study was conducted to investigate the value of *Synechococcus* 7942 (Syne) as a sensitizer for photo-sonodynamic therapy (PSDT). Syne was characterized. The efficacy of Syne-mediated PSDT were verified *in vitro* (in 4T1 breast cancer cells) and *in vivo* (in a breast tumor-bearing mouse model). The safety of Syne-mediated PSDT was verified *in vivo.* Results indicated that Syne triggered the generation of oxygen and ROS during PSDT, thereby inducing cell death in 4T1 cells. Syne-mediated PSDT induced the death of tumor cells both *in vitro* and *in vivo.* The speed of tumor growth was delayed in animals receiving PSDT. Syne-mediated PSDT was more effective than photodynamic therapy or sonodynamic therapy alone. In addition, administration of a Syne monomer resulted in satisfactory tumor targeting. Syne-mediated PSDT affected neither the animal body weight nor the major organs, indicating satisfactory safety. Accordingly, Syne is an efficient, safe, and readily available sensitizer that is ideal for potential clinical use of PSDT to treat breast cancer. The findings of this study are useful for exploration of a novel sensitizer for PSDT, which might be a promising alternative therapy against breast cancer.

Keywords sensitizer, *Synechococcus* 7942 (Syne), photo-sonodynamic therapy (PSDT), breast cancer

1. Introduction

Breast cancer is the most common malignancy among women and stands as the second leading cause of tumor-related death in women. Nevertheless, conventional strategies thus far, such as surgery, radiotherapy, and chemotherapy, have not achieved satisfactory efficacy, particularly in patients with cancer at an advanced stage. Due to the knotty nature of treatments against breast cancer, many alternative treatments were considered, and photodynamic therapy (PDT), sonodynamic therapy (SDT), and photo-sonodynamic therapy (PSDT, a combination of PDT and SDT) have garnered considerable attention (*1*).

PDT is a non-invasive cancer therapy based on generation of reactive oxygen species (ROS) triggered by activation of photosensitized agents with specific wavelengths of light. Use of PDT alone has many limitations, such as limited penetration (often less than 1 cm), uncertain efficacy, potential damage to normal cells, and the generation of tolerance in targeted cells (*1*), which have further limited the use of PDT. SDT is another therapy that is also based on the generation of ROS. It has satisfactory penetration (often more than 8 cm) and less damage to normal cells/tissues (*1*). Due to the deep penetration and greater focusing of ultrasound, SDT is often combined with PDT to provide a more practical PSDT for use in cancer treatment. Early in 2000, Zhao *et al*. reported that combined use of PDT and SDT resulted in tumor necrosis approximately 2-3 times deeper than use of either therapy alone in mice with squamous cell carcinoma of the skin (*2*). PSDT has been used to treat breast cancer. Liu *et al*. used composite peptide amphiphile-indocyanine green (ICG) nanomicelles in conjunction with a sono-/photosensitizer of ICG encapsulation for combined SDT, PDT, and photothermal therapy (PTT). They found that this treatment had ideal efficacy in both *in vivo* and *in vitro*

breast cancer models (*3*). Zheng *et al*. used a carrier-free nanosensitizer, oleanolic acid (OC), consisting of an anti-cancer drug, oleanolic acid, and a photosensitizer, chlorin e6 (Ce6), to treat orthotopic 4T1 breast tumor-bearing mice. They found that self-assembled carrier-free nanosensitizer OC satisfactorily mediated the efficacy of PSDT to treat breast cancer-bearing mice (*4*). Moshfegh *et al*. used hematoporphyrin as a sensitizer for PSDT, and they found that hematoporphyrin-mediated PSDT delayed tumor growth (*5*). Learning from these previous studies, we understand that selection of an ideal sensitizer might play a vital role in achieving efficacious PDT, SDT, and PSDT.

An ideal sensitizer for PDT, SDT, and particularly for PSDT should have several characteristics: *i*) It should have satisfactory biocompatibility so it can thus be used in both PDT and SDT (good as both a photosensitizer and sonosensitizer). Importantly, it should enhance the synergistic effects of PDT and SDT. *ii*) It should have the ability to trigger the generation of ROS. *iii*) It has good solubility and aggregation to avoid ROS quenching (*6*). *iv*) Its safety and efficacy can be verified. *v*) It should be easily synthesized or produced (ready availability). To have these characteristics, sensitizers were often modified using nanotechnology-based technologies in particular. So far, several modified sensitizers for PSDT to treat breast cancer have been reported, such as OC (*4*), Ce6 (*4,7*), hematoporphyrin (*5*), cationic morpholino-phthalocyanines conjugated to nitrogen and nitrogen-sulfur doped graphene quantum dots (*8*), and sinoporphyrin sodium (DBDMS) (*9*). However, all of these sensitizers have their special advantages and weaknesses. Accordingly, exploration of a novel sensitizer for PSDT to treat breast cancer is an indispensable task for researchers. Cyanobacteria, a group of non-pathogenic bacteria, are coming into the picture due to their capacity to produce large volumes of oxygen (*10*). A previous study by our laboratory found that *Synechococcus* 7942 (Syne), a cyanobacterium, mediated the efficacy of PDT to treat breast cancer by relieving tumor hypoxia and enhancing the generation of ROS (*11*). Moreover, Syne is moderately effective at immune stimulation. Hence, Syne has been identified as a good photosensitizer for PDT (*11*). Based on the findings of the previous study, we hypothesized that Syne is also a good sonosensitizer that could display anti-tumor action in PSDT as well. We therefore conducted the current study to verify whether Syne can exhibit its efficacy as a sensitizer for PSDT in breast cancer models. We believe the findings of the current study will facilitate for exploration of novel sensitizers for PSDT, which is an important promising alternative therapy against breast cancer.

2. Materials and Methods

2.1. Materials and animals

Syne was purchased from the freshwater algae seed bank of the Institute of Aquatic Biology (FACHB, Wuhan, China). 4T1 breast cancer cells were obtained from the cell culture bank of the Chinese Academy of Sciences (CAS, Shanghai, China).

A total of 42 BALB/c mice (female, 6 weeks old, weighing 15–18 g, Beijing Charles River Laboratory Animal Technology, Ltd, Beijing, China) were used in this study. Mice were raised under conditions of 60% humidity, room temperature of 23°C, and a 12-h light-dark rhythm (7:00 AM–7:00 PM) with food and water freely available.

They were treated in strict compliance with the National Institutes of Health Guidelines for the Care and Use of Laboratory Animals. All experiments were approved of and supervised by the Animal Ethics Committee of the Shenzhen Third People's Hospital (approval number 2022-018)

2.2. Experimental design

Experiments included the confirmation of the characterization of Syne, evaluation of Syne-related photosynthetic oxygen production and photo-sonodynamic effects, and verification of the efficacy of Syne in photo-sonodynamic treatments *in vitro* and *in vivo*. The protocol for this study is shown in Figure 1.

2.3. Conformation of the characterization of Syne

Syne solution samples were subjected to UV-visible spectrophotometry (B-600 Ultra-micro–UV Spectrophotometer, METASH, China). Absorbance was configured to confirm the absorption peaks of Syne solutions.

2.4. Evaluation of Syne-related photosynthetic oxygen production and photo-sonodynamic effects

Oxygen production by Syne solutions at concentrations of 1, 2.5, 5, and 10 $\times 10^7$ CFU/mL in 30 min, as well as at times of 0, 10, 20, 30, 40, 50, 60 min at 1×10^8 CFU/mL was detected using a dissolved oxygen meter (S4 -Standard Kit, METTLER TOLEDO, Shanghai, China). The probe of the oxygen-dissolving instrument was inserted into the Syne solutions, and the dissolved oxygen levels were measured in real time. Wavelength was selected as λ = 660 nm in light of a previous study (*11*). ROS production was detected with a 2′,7′-dichlorofluorescence diacetate (DCFH-DA) probe (Sigma, St. Louis, USA) ex/em: λ = 485/525 nm.

Then, 2 mL of each Syne solution (10 $\times 10^7$ CFU/mL) was placed into five dishes, mixed with 10 μL of DCFH-DA, and treated user the following conditions. The Syne group was the control without any treatment. The Syne + US group was treated with an ultrasound probe (1.0 W/cm2, 50% duty cycle, XK-2011R, Xingkang Ltd,

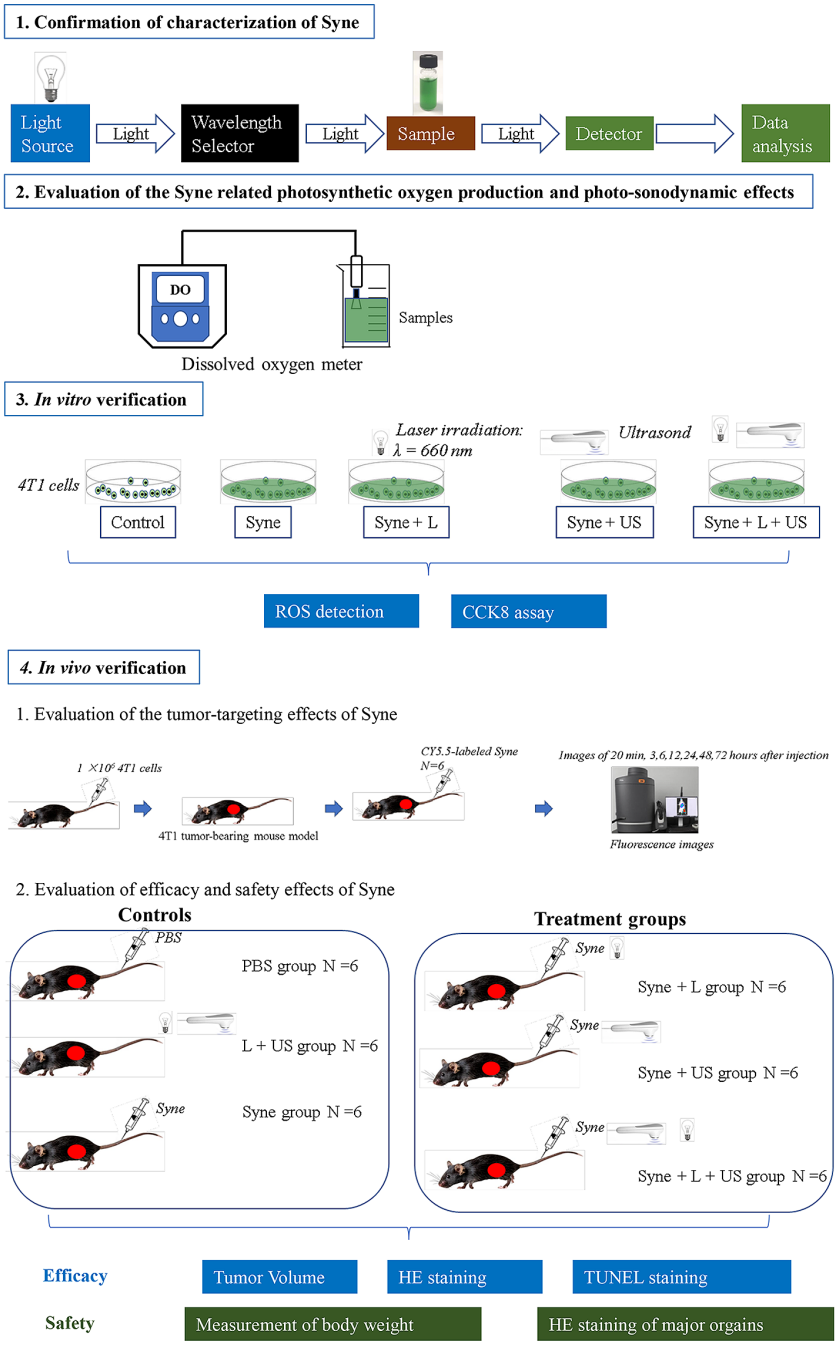

Figure 1. Protocol of the current study.

Wuhan, China) for 8 min. The Syne + L + US group was treated with laser irradiation (λ = 660 nm, LWRL, Laserwave, Beijing, China) for 1 min followed by the aforementioned ultrasound treatment. After the initiation of the treatments, a 100-μL sample of the Syne solution was extracted every minute from each group and placed into a 96-well plate. The fluorescence intensity of each well was observed and measured using a microplate reader (Model, Biotek Instruments, Vermont, USA)

2.5. *In vitro* verification of the efficacy of Syne in photo-sonodynamic treatments

4T1 breast cancer cells were seeded in 96-well plates and incubated in 37°C, 5% CO_2 for 24 h. When the cells covered approximately 80% of the plate bottom, they could be used for subsequent experiments. Then, cells were divided into 5 groups. The Control group was the intact 4T1 cells (1×10^4 cells/well) with distilled water and incubated at 37°C in 5% CO_2 for 3 h. Syne-related groups were prepared by incubating Syne (1×10^7 CFU/mL) with 4T1 cells (1×10^4 cells/well) at 37°C in 5% CO_2 for 3 h for subsequent experiments. The Syne group was only the Syne solution without any treatments. The Syne + L group was treated with laser irradiation (λ = 660 nm) for 1 min. The Syne + US group was treated with an ultrasound probe (1.0 W/cm^2, 50% duty cycle, XK-2011R, Xingkang Ltd, Chengdu, China) for 3

min. The Syne + L + US group was treated with laser irradiation followed by ultrasound treatment with the aforementioned parameters. After the treatments, all samples were incubated at 37℃ in 5% CO_2 for 24 h for subsequent CCK8 assays. Each group included at least 5 wells for repetition of the experiments.

A conventional CCK8 assay was used to assess cellular viability. For preparation of the CCK8 reagent, 10 μL of the original CCK8 solution (Beyotime, Shanghai, China) was mixed with 90 μL of 1640 medium. This mixture was added to a well, and cells in each group (1×10^4 cells/well) were incubated at 37℃ in 5% CO_2 for 10 min. Fluorescence images of ROS generation were obtained by confocal microscopy (SpinSR, Olympus, Tokyo, Japan). Absorbance was measured at a wavelength of 450 nm using an enzyme meter. The optical density (OD) values of each well were recorded, and the cell viability in each group was calculated using the formula: Cell viability (%) = (OD treatment group - OD blank group) / (OD control group - OD blank group) × 100%.

DCFH-DA and Hoechst staining were also performed to check the generation of ROS and the nucleus of 4T1 cells. Analogous with the aforementioned experiments measuring ROS generation, 4T1 cells (2×10^4 cells per well) were cultured in an 8-well culture chamber. When the cells covered 80% of the chamber, they were used for subsequent experiments. For the Syne-related groups, Syne (1×10^7 cells/mL) was added to the cells, and the mixture was incubated for 3 h. Then, the supernatant was discarded and 200 μL of fresh culture medium containing 10 μL DCFH-DA (1 mg/mL) was added, and the mixture was incubated for 30 min. Then, cells were grouped and treated as described earlier. After the treatments, cells were incubated for 2 h and washed with PBS twice. Then, fresh medium containing Hoechst 33258 was added, and cells were stained for 30 min. Fluorescence images of ROS generation were obtained by confocal microscopy (CLSM) to determine the amount of ROS. The average fluorescence intensity of the fluorescence images was semi-quantitatively analyzed using the software ImageJ (ImageJ1.51K, NIH, USA).

For viability/cytotoxicity assay, all groups of cells after treatments were returned to the incubator and incubated at 37°C in 5% CO_2 for 21 h. Then, the cells were incubated with prepared Calcein and propidium iodide (PI) in the dark for 1 hour. Cell staining was examined using a fluorescence microscope (BZ-X800E, Keyence, Tokyo, Japan, ex/em: λ = 545/605 nm).
Semi-quantitative analyses were also performed to calculate the ROS intensity, cell viability, and PI intensity.

2.6. *In vivo* verification of the efficacy and safety of Syne in photo-sonodynamic treatments

Anesthetized with isoflurane in a special chamber exposed to 5% isoflurane mixed with 95% O_2 for 4 min (*12*), 42 BALB/c mice were injected with 4T1 cells (1×10^7 cells/mL, 0.1 mL) on the outer posterior side of the right lower limb root to create the breast tumor-bearing mouse model. After the injection, animals were returned to normal conditions. Once the tumor grew to experimental size (approximately 0.1 cm^3), animals were used in subsequent experiments.

Six mice were used to confirm tumor targeting by Syne. Twenty μL of Cy5.5 (10 mM, 1 mL in DMSO, Thermo Fisher Scientific, USA) was added to the Syne solution (5×10^8 CFU/mL, 2mL), and the mixture was incubated for 60 min at room temperature. Then, the solutions were adjusted to 5×10^8 CFU/mL to prepare the CY5.5-labeled Syne solutions. CY5.5-labeled Syne (0.1 mL) was injected into the animals *via* the tail vein. After injection of the CY5.5-labeled Syne for 20 min, animals were anesthetized with isoflurane and placed into a fluorescence imager for small animals (IVIS, Caliper Life Sciences, USA) to observe the distribution and accumulation of Syne over time. Data were recorded at 7 time points, namely 20 min, 3, 6, 12, 24, 48, and 72 h after injection.

The remaining animals were divided into 6 groups (n = 6 for each group): The Control groups included 3 groups, namely the PBS group (injection of 0.1 mL of PBS *via* the tail vein), the L + US group (animals underwent laser irradiation followed by ultrasound treatment), the Syne group (injection of Syne *via* the tail vein), the Syne + L group (injection of Syne and treatment with laser irradiation), the Syne + US group (injection of Syne and treatment with ultrasound), and the Syne + L + US group (injection of Syne and treatment with laser irradiation followed by ultrasound treatment). Parameters for treatments were: injection of Syne (0.1 mL, 5×10^8 CFU/mL); laser irradiation (λ = 660 nm, 0.1 W/cm^2, 30 min); and ultrasound treatment (1.0 W/cm^2, 50% duty cycle, 5 min). Tumor size and body weight were monitored for 16 days. Standard hematoxylin and eosin (HE) staining was used to check for changes in the major organs (heart, liver, spleen, lungs, and kidneys) of animals after observation for 16 days. In addition, HE staining and TUNEL staining were also used to compare the tumor in the PBS group and the Syne + L + US group. Animals were euthanized by asphyxiation with CO_2, and the major organs (heart, liver, spleen, lungs, and kidneys) were removed and fixed with 4% paraformaldehyde for 1 h and then dehydrated with a sucrose solution. Then, the organs were placed in optimal cutting temperature medium (Sakura Tissue Tek, West Chester, PA) overnight at −80 °C. A Leica cryomicrotome (CM1510, Leica Nussloch, Germany) was used to make frozen sections (6 μm), which were subjected to HE and TUNEL staining. For HE staining, the frozen sections were washed in water and stained in hematoxylin for 2 min. Then, the slides were rinsed in 95% ethanol and stained with eosin for 10 sec and washed with tap water.

The remaining slides were subjected to TUNEL staining. Slides were washed with PBS and placed in 0.1% Triton X-100 and 0.1% sodium citrate for 2 min on ice. Then, slides were incubated with TUNEL reaction mixture with deoxyribonucleotide transferase (TdT) and the fluorescent label (tetramethlylrhodamine-conjugated nucleotides) in a humidified chamber in the dark for 1 hour at 37℃. After slides were washed with PBS, they were mounted with 50% glycerin in PBS. All of the stained slides were observed with a microscope (BX53, Olympus, Tokyo, Japan)

2.7. Statistical analysis

The software GraphPad Prism (V8.0.2, GraphPad Software, MA, USA) was used for statistical analysis. The normal distribution of experimental data was checked using the Kolmogorov-Smirnov test. Data are expressed as the mean ± standard deviation. A two-tailed analysis of variance (ANOVA) with Tukey post-hoc correction was used for multi-comparisons. Each experiment was repeated at least 3 times, and the results were averaged. $P < 0.05$ was considered to be a significant difference.

3. Results

3.1. Characterization of Syne

UV-visible spectrophotometry indicated that Syne exhibited relatively strong absorption peaks at 631 nm and 683 nm (Figure 2), which confirmed that the Syne used in this study was activated by strong near-infrared light and enabled photosynthetic oxygen production (*13*).

3.2. Evaluation of Syne-related photosynthetic oxygen production and its photo-sonodynamic effects

Figure 3 shows the results of verifying Syne's photosynthetic oxygen production and photo-sonodynamic effects. Oxygen bubbles were observed when the Syne solution was irradiated with laser light (λ = 660 nm, Figure 3A). With increasing concentrations of Syne, the release of oxygen increased accordingly (Figure 3B). With an increasing irradiation time, the release of oxygen increased accordingly (Figure 3C). The FCFH-DA FL intensity ratio increased over time. Results were Syne + L + US > Syne + US > Syne (Figure 3D). These results confirmed the photosynthetic oxygen production and photo-sonodynamic effects of the Syne solution used in this study.

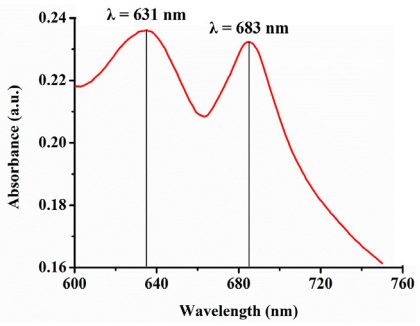

Figure 2. Data from UV-visible spectrophotometry.

3.3. Verification of the efficacy of Syne in photo-sonodynamic treatments *in vitro*

Figure 4 shows the efficacy of photo-sonodynamic treatments with Syne *in vitro*. Compared to the control, the four groups stained green, indicating the generation of ROS. The volume of ROS production was Syne + L + US > Syne + US > Syne + L > Syne (Figure 4A). Semi-quantitative analyses confirmed that production of ROS in the Syne + L + US group was significantly higher than that in the other groups ($p < 0.05$, Figure 4B). In terms of the cellular viability of breast cancer cells assessed with a CCK8 assay, 61% of cells in the Syne + L + US group died. The cellular survival rates were control > Syne > Syne + L > Syne + US > Syne + L + US, where Syne + L + US was the lowest ($p < 0.001$, *vs.* Syne + US group, Figure 4C). In terms of cellular cytotoxicity, PI intensity (red, dead cells) was Syne + L + US > Syne + US > Syne + L > Syne ($p < 0.001$, *vs.* Syne + US group, Figures 4D, E), indicating that cytotoxic effects were strongest in the Syne + L + US group. These experiments yielded similar results, namely the efficacy against

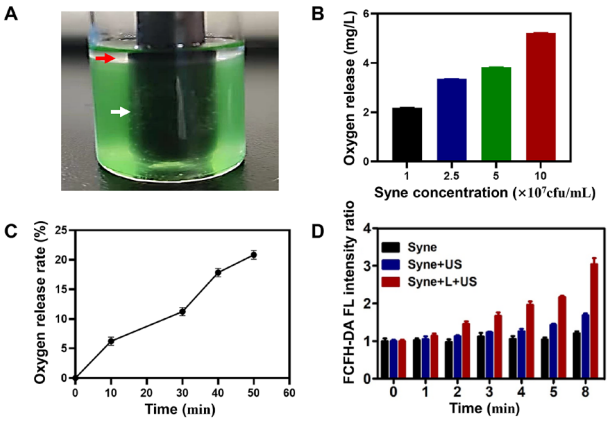

Figure 3. Verification of the photosynthetic oxygen production by and photo-sonodynamic effects of Syne solutions. (A), Oxygen bubbles appeared once the Syne solution was irradiated with a laser light (λ = 660 nm). The white arrow points to oxygen bubbles, and the red arrow points to an ethyl acetate layer at the top of solution. **(B)**, Release of oxygen increased in Syne solutions with increasing concentrations (1–10 × 10^7 CFU/mL) when they were irradiated for 30 min under a laser light (λ = 660 nm). **(C)**, Release of oxygen increased with the increasing irradiation time (0–60 min) when a Syne solution (1 × 10^8 CFU/mL) was irradiated under a laser light (λ = 660 nm). **(D)**, Verification of the photo-sonodynamic effects on the Syne solutions (1 × 10^8 CFU/mL) which were used in ultrasonic therapy (Syne + US, 1.0 Wcm^{-2}, 50% duty cycle, 8 min) or ultrasonic therapy with laser irradiation (Syne + L + US, 660 nm laser irradiation, 8 min). An intact solution (Syne) was used as the control.

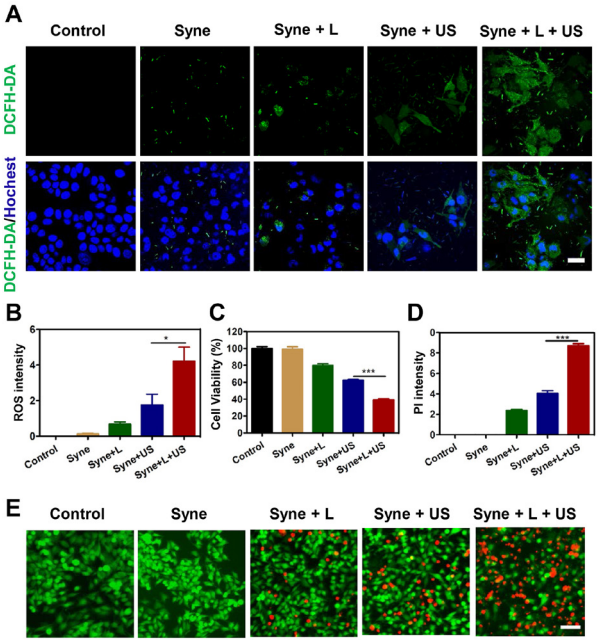

Figure 4. Evaluation of the efficacy of photo-sonodynamic treatments involving Syne *in vitro*. (A), Generation of singlet oxygen by different treatments involving Syne according to ROS staining. ROS are in green, and Hochest+ 4T1 cells are in blue. Bar = 20 μm. **(B)**, Semi-quantitative analysis of ROS average fluorescence intensity in different groups. **(C)**, Cell viability of 4T1 cells in different groups (n = 3). **(D)**, Semi-quantitative analysis of average PI fluorescence intensity in different groups. **(E)**, CLSM of 4T1 cells stained with Calcein-AM (green) and PI (red) as a result of different treatments involving Syne, Bar = 50 μm. Syne + L = laser irradiation, Syne + US = ultrasonic therapy, Syne + US + L = laser irradiation + ultrasonic therapy. Data = mean ± standard deviation, *means $p < 0.05$, ***means $p < 0.001$.

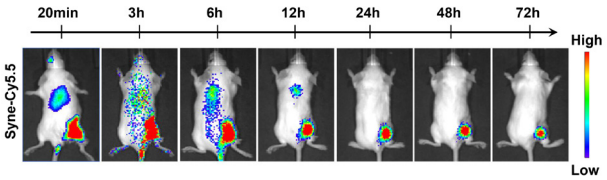

Figure 5. Confirmation of the delivery of tumor-targeting Syne with Syne-Cy5.5 fluorescence images in 4T1 tumor-bearing mice.

breast cancer cells was Syne + L + US > Syne + US > Syne + L. Accordingly, the strongest efficacy of photo-sonodynamic treatments was verified *in vitro*.

3.4. Verification of the efficacy of Syne in photo-sonodynamic treatments *in vivo*

Figure 5 shows the tumor targeting by Syne in a breast tumor-bearing mouse model. The fluorescence signal was detected throughout the body after administration of CY5.5-labeled Syne *via* the tail vein. Then, the labeled Syne gradually distributed and accumulated around the tumor over time. These results indicated that Syne satisfactorily targeted tumors and could be potentially used in subsequent photo-sonodynamic treatments (Figure 5).

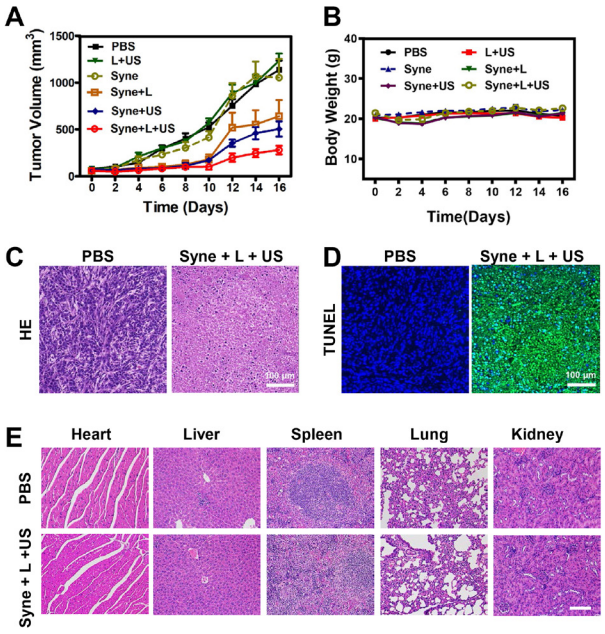

Figure 6. Verification of the efficacy of Syne in photo-sonodynamic treatment of tumors *in vivo*. (A), Data on tumor volumes (n = 6). **(B)**, Body weight of animal subjects (n = 6). **(C)**, Representative images of HE staining of tumor sections. **(D)**, Representative images of TUNEL staining of tumor sections. **(E)**, Representative images of HE staining of sections of major organs. Bar = 100 μm.

Figure 6 shows the efficacy and safety of Syne in treating the breast tumor-bearing mice. Tumor volume increased over time. Tumor growth was slowest in the Syne + L + US group. The speed of tumor growth was non-Syne groups (PBS, L + US, Syne) > Syne + L > Syne + US > Syne + L + US (Figure 6A). The results of HE staining (Figure 6C) and TUNEL staining (Figure 6D) indicated a large amount of cell death and histological disintegration in the Syne + L + US group (*vs.* PBS group). This verified the apoptosis and necrosis of tumor lesions induced by Syne + L + US treatment.

In terms of safety, the body weights of animals in each group did not change during the 16-day treatments, indicating that treatments had negligible toxicity (Figure 6B). Moreover, examination of the HE stained images of major organs in the treatment groups, including the heart, liver, spleen, lungs, and kidneys, revealed no significant histopathological lesions. The safety of photo-sonodynamic treatment was therefore verified (Figure 6E).

4. Discussion

The current study verified the value of Syne as a sensitizer for PSDT to treat breast cancer in 4T1 breast cancer cells and a breast tumor-bearing mouse model. Experiments *in vitro* indicated that Syne had the capacity to trigger the generation of oxygen and ROS during PSDT, thereby inducing cell death in 4T1 cells. *in vivo* results revealed ideal efficacy and safety when animals underwent PSDT. The current results suggest that Syne

is an ideal photosensitizer and sonosensitizer that may mediate efficacious PSDT in treating animals with breast cancer. To the extent known, this is the first study to evaluate the value of Syne as a sensitizer for PSDT. The findings of the current study are useful for further developing Syne-mediated PSDT as an alternative therapy to treat breast cancer.

4.1. Characterization of Syne

When irradiated with laser light (λ = 660 nm), Syne significantly triggered the generation of oxygen (Figures 3A-C). This effect was dose-dependent (Figure 3B) and time-dependent (Figure 3C), indicating that Syne can serve as a photosensitizer. These results agree with those of a previous study (*11*). A time-effect relationship was evident in the Syne + US group (Figure 4C), indicating that Syne also can be used as a sonosensitizer. Efficacy was significantly higher in the Syne + L + US group than in the Syne + US group, indicating a remarkable synergistic effect of PDT and SDT (Figure 3D). Thus, Syne is an ideal sensitizer for PSDT. In addition, these experiments were performed using the Syne monomer without any modification like integration with nanoparticles, which suggests that Syne itself can be used directly as a sensitizer in subsequent experiments without sophisticated modifications.

4.2. Verification of the efficacy of Syne in PSDT *in vitro*

When 4T1 breast cancer cells were used, Syne triggered the generation of ROS (Figures 4A, B) and induced the death of tumor cells (Figures 4A, C-E) as part of Syne + L, Syne + US, and Syne + L + US. In addition, the effect intensity was Syne + L + US (PSDT) > Syne + US (SDT) > Syne + L (PDT) > Syne (Control). These results confirmed that Syne was efficacious in combined PDT and SDT, and this efficacy was significantly better than that of PDT or SDT alone. Moreover, results seem to imply that the tumor cells were more sensitive to SDT (*vs.* PDT) mediated by Syne. These results differed from those of previous studies in which therapy was mediated by Ce6 (*14*) and DBDMS (*9*), which indicated that cells were more sensitive to PDT (*vs.* SDT). A plausible interpretation might be that the sensitivity of PDT and SDT varies with different sensitizers. This issue warrants further investigation in the future.

4.3. Verification of the efficacy of Syne in PSDT *in vivo*

Results suggested that Syne satisfactorily targeted tumors without any complicated processes such as integration with nanoparticles (Figure 5). Importantly, this confirmed the satisfactory availability of Syne. It is easy to prepare and produce in comparison to the previously reported sensitizers. Thus, Syne is a good candidate for future clinical use. In terms of efficacy, Syne-mediated PDST resulted in the slowest tumor growth, and the speed of tumor growth was Syne + L > Syne + US > Syne + L + US (Figure 6A). These results were in accordance with the current results *in vitro*, confirming that Syne mediated the efficacy of SDT > PDT. Moreover, HE staining (Figure 6C) and TUNEL staining (Figure 6D) indicated that PSDT was efficacious against tumor cells *in vivo*. In terms of safety, PSDT mediated by Syne did not affect the body weight (Figure 6B) and major organs (Figure 6E) of the animal subjects. Accordingly, the safety and efficacy of PDST mediated by Syne were verified.

4.4. Limitations

This study had several limitations that might have led to biased conclusions: *i*) The sample size of animals in each group was too small, and *ii*) The effects of Syne + US + L (SPDT) were not evaluated since previous studies revealed marked differences between PSDT and SPDT (*9,14*). All of these limitations will be addressed in subsequent studies.

5. Conclusions

The current study characterized Syne and it investigated the efficacy and safety of Syne-mediated PSDT to treat breast cancer *in vitro* and *in vivo*. Results indicated that Syne is effective at triggering the generation of ROS. Syne-mediated PSDT exhibited satisfactory efficacy against 4T1 breast cells and in a breast tumor-bearing mouse model. The safety of Syne-mediated PSDT was also verified. Moreover, Syne exhibited ideal availability since it did not require sophisticated modifications. Accordingly, Syne is an efficient, safe, and readily available sensitizer, which is ideal for potential clinical use in PSDT to treat breast cancer.

Funding: This work was supported by the National Key R&D Program of China (nos.: 2023YFA0915600, 2023YFC2308300), the Natural Science Foundation of China (nos.: 82372271 and 22107045), Key Area Projects for Universities in Guangdong Province (no.: 2022DZX2022), the Guangdong Provincial Key Laboratory of Advanced Biomaterials (no.: 2022B1212010003), the Shenzhen Science and Technology Program (nos.: JCYJ20220530163005012, JCYJ20210324115611032, and JCYJ20210324132012035), the Shenzhen Clinical Medical Center for Emerging infectious diseases (no.: LCYSSQ20220823091203007), the Shenzhen Clinical Research Center for Tuberculosis (no.: 20210617141509001), the Shenzhen High-level Hospital Construction Fund (nos.: 23274G1001, 23250G1005, 24250G1027, and 24250G1019), and the National Cancer Center/National Clinical Research Center for Cancer/ Cancer Hospital & Shenzhen Hospital, Chinese Academy

of Medical Sciences and Peking Union Medical College, Shenzhen (nos.: E010221005 and CFA202201006).

Conflict of Interest: The authors have no conflicts of interest to disclose.

References

1. Hu H, Zhao J, Ma K, Wang J, Wang X, Mao T, Xiang C, Luo H, Cheng Y, Yu M, Qin Y, Yang K, Li Q, Sun Y, Wang S. Sonodynamic therapy combined with phototherapy: Novel synergistic strategy with superior efficacy for antitumor and antiinfection therapy. J Control Release. 2023; 359:188-205.
2. Jin ZH, Miyoshi N, Ishiguro K, Umemura S, Kawabata K, Yumita N, Sakata I, Takaoka K, Udagawa T, Nakajima S, Tajiri H, Ueda K, Fukuda M, Kumakiri M. Combination effect of photodynamic and sonodynamic therapy on experimental skin squamous cell carcinoma in C3H/HeN mice. J Dermatol. 2000; 27:294-306.
3. Liu Z, Li J, Chen W, Liu L, Yu F. Light and sound to trigger the Pandora's box against breast cancer: A combination strategy of sonodynamic, photodynamic and photothermal therapies. Biomaterials. 2020; 232:119685.
4. Zheng Y, Li Z, Yang Y, Shi H, Chen H, Gao Y. A nanosensitizer self-assembled from oleanolic acid and chlorin e6 for synergistic chemo/sono-photodynamic cancer therapy. Phytomedicine. 2021; 93:153788.
5. Moshfegh S, Jadidi M, Hasanzadeh H, Nasr R, Mirmohammadkhani M. Efficacy of Hematoporphyrin mediated photo-sonodynamic therapy on mice breast cancer. Intl J Rad Res. 2022; 20:555-561.
6. Yang Y, Fan Z, Zheng K, Shi D, Su G, Ge D, Zhao Q, Fu X, Hou Z. A novel self-targeting theranostic nanoplatform for photoacoustic imaging-monitored and enhanced chemo-sonodynamic therapy. J Mater Chem B. 2021; 9:5547-5559.
7. Sun D, Zhang Z, Chen M, Zhang Y, Amagat J, Kang S, Zheng Y, Hu B, Chen M. Co-immobilization of Ce6 sono/photosensitizer and protonated graphitic carbon nitride on PCL/gelation fibrous scaffolds for combined sono-photodynamic cancer therapy. ACS Appl Mater Interfaces. 2020; 12:40728-40739.
8. Nene LC, Nyokong T. Photo-sonodynamic combination activity of cationic morpholino-phthalocyanines conjugated to nitrogen and nitrogen-sulfur doped graphene quantum dots against MCF-7 breast cancer cell line *in vitro*. Photodiagnosis Photodyn Ther. 2021; 36:102573.
9. Liu Y, Wang P, Liu Q, Wang X. Sinoporphyrin sodium triggered sono-photodynamic effects on breast cancer both *in vitro* and *in vivo*. Ultrason Sonochem. 2016; 31:437-448.
10. Cohen JE, Goldstone AB, Paulsen MJ, *et al*. An innovative biologic system for photon-powered myocardium in the ischemic heart. Sci Adv. 2017; 3:e1603078.
11. Liu L, He H, Luo Z, Zhou H, Liang R, Pan H, Ma Y, Cai L. In situ photocatalyzed oxygen generation with photosynthetic bacteria to enable robust immunogenic photodynamic therapy in triple-negative breast cancer. Advanced Functional Materials. 2020; 30:1910176.
12. Gielis JF, Jungraithmayr W, Boulet GA, Bogers JP, Weder W, Cos P, Van Schil PEY. A murine model of lung ischemia and reperfusion injury: Tricks of the trade. J Surg Res. 2015; 194:659-666.
13. Fushimi K, Narikawa R. Cyanobacteriochromes: Photoreceptors covering the entire UV-to-visible spectrum. Curr Opin Struct Biol. 2019; 57:39-46.
14. Wang P, Li C, Wang X, Xiong W, Feng X, Liu Q, Leung AW, Xu C. Anti-metastatic and pro-apoptotic effects elicited by combination photodynamic therapy with sonodynamic therapy on breast cancer both *in vitro* and *in vivo*. Ultrason Sonochem. 2015; 23:116-127.

Received July 24, 2024; Revised August 14, 2024; Accepted August 18, 2024.

[§]These authors contributed equally to this work.
**Address correspondence to:*
Xin Kuang, Department of Anesthesiology, People's Hospital of Longhua, 38 Jinglong construction Road, Shenzhen, Guangdong Province 518109, China.
E-mail: kx6924@126.com

Tetsuya Asakawa, Mingbin Zheng, and Pengfei Zhao, Institute of Neurology, National Clinical Research Center for Infectious Diseases, Shenzhen Third People's Hospital, 29 Bulan Road, Shenzhen, Guangdong Province 518112, China.
E-mail: asakawat1971@gmail.com (TA), mingbinzheng@126.com (MZ), pengfeizhao@aliyun.com (PZ)

Released online in J-STAGE as advance publication August 22, 2024.